International Journal of Innovations in Engineering and Technology (IJIET)
http://dx.doi.org/10.21172/ijiet.142.10

Estimating Asphalt Pavement Damaged-Area from Onsite Survey and Laboratory Test Data by Neural Network Model

Tienfuan Kerh[1], Shu-Rong Yang[2], Yi-Wen Lai[3]
[1,2,3]*Deparment of Civil Engineering , National Pingtung University of Science and Technology Pingtung 91201, Taiwan*

Abstract- Damage of asphalt pavement may cause a problem to endanger road users, as that the issues related to road pavements are of great importance to the maintenance of traffic safety. This study initially investigates the damaged-area of asphalt concrete road surface and the number of traffic volume equivalent of 41 sites for a specified highway section in Taiwan. Then, by taking asphalt pavement samples onsite to obtain three parameters, including asphalt compaction, bitumen content, and asphalt viscosity from laboratory test. Finally, by using the simple and effectiveness characteristics of artificial neural network, a series of models are developed for linking the road surface damage-area and the combination of the other parameters. Three indices, including correlation coefficient, mean square error, and efficiency coefficient, are used to evaluate the performance of model developed. The comparison results showed that the model of using back-propagation network with Levenberg-Marquardt optimization, could achieve a better performance than that of using cascade-forward network with Bayesian regularization. The proposed new method in this study may be applicable to other road regions of interest, and the results might provide useful information for relevant government agencies in traffic safety management.

Keywords – Asphalt concrete road, traffic equivalent volume, asphalt property, pavement damaged-area

I. INTRODUCTION

Without a doubt, the majority of road surfaces for a highway system are paved by asphalt concrete in modern countries. The quality of a road pavement can significantly affect the comfort level for road users, as well as it plays an important role for road maintenance and traffic safety management. In particular, the traffic safety problem due to road surface damage may require pay more attention as it usually involves life and property losses. Based on previous report, there are about 171 state compensations claimed per year in average from official statistics of Ministry of Transportation and Communications, Taiwan [1]. Therefore, the issues related to road surface damage are crucial and can be studied either from academic or practical standpoint.

The asphalt concrete pavement may be damaged by various reasons such as climate, traffic volume, and pavement mixtures, which results in the reducing of road service length and service quality. In general, the damage forms of an asphalt concrete pavement may include splitting, disintegration, distortion, rutting, and fatigue cracking [2]. Certainly, the traffic volume can direct affect pavement damage, but the pavement mixtures; that is, the asphalt content and aggregate ratio may also have an influence on the road surface damage. It is understand that too less asphalt content may cause pavement-aging problem; on the other hand, the phenomenon of pavement bleeding may occur due to too much asphalt content in the mixture [3-4]. By any means, the shear strength of the road becomes weaken, and that may bring on rutting, squeezing, or waving type of pavement damages. In addition, the viscosity of asphalt concrete can use to evaluate the ability of flow resisting, and it can affect the stability of a road surface. The compactness of asphalt concrete can affect the strength, stiffness, and flatness of a road foundation. All of these factors may have a relationship with pavement-damaged area.

In accordance with ASTM D6433-03, the damaged-area is one of key factors to classify the severity level of a pothole for an asphalt concrete pavement [5]. Indeed, one can use some of advanced equipment to measure the damaged-area of an asphalt concrete pavement. For instance, the quadcopter unmanned aerial vehicle with a digital camera, can be taken to precisely analyze pavement damaged-area [6]. The pavement crack and pothole can be detected from a recognition system for mobile android-based devices [7]. Additionally, the pavement damaged-area can be recognized and predicted from the difference between background pixel and crack pixel in a gray-scaled road surface graph [8]. However, the straightforward and economical way to obtain the damaged-area of an asphalt concrete pavement is by calculating the shape and size from onsite surveys.

There are many previous literatures have been published to explore the damage of asphalt concrete pavement (e.g. [9-18]), but most of studies are focused on finding damage characteristics, reasons, and mechanism of asphalt pavement by different approaches. It is difficult to find a study for predicting pavement damaged-area from various asphalt parameters. Therefore, the aim of this study is to develop a model by using neural network approach for

linking pavement damaged-area from onsite measurement with laboratory testing data, including asphalt compactness, asphalt content, and asphalt viscosity. Furthermore, the factor of a statistical traffic volume equivalent is also considered in the neural network model. From a series of model training and comparison, a relatively better model is developed according to the evaluation indices of determination coefficient, mean square error, and efficiency coefficient. The method used in this study may provide a simple way to predict pavement damaged-area, which may help to identify potential hazardous region or provide information for improving road traffic safety.

II. ONSITE SURVEY AND LABORATORY TESTING DATA

2.1 Investigation Area

As shown in Figure 1 is the research road section in the present study, where this road section starting from 423 K+003 to 463 K+225, a total of about 40 km, is part of TAI1 line, one of important state highways in the island of Taiwan. As this road section is the major way to Kenting National Park (KNP), the car discharge is relatively heavy [19]. The traffic flow includes various type of vehicles such as big buses, big trucks, tractor-semi trailers, compact cars, and motorcycles, where the motorcycles accounted for the most. Since it will become complicate, by considering each type of cars in traffic flow analysis for the 41 survey locations as seen in the figure, thus the passenger car equivalent (PCE) is taken to calculate traffic volume, and that becomes one of input parameters in this study.

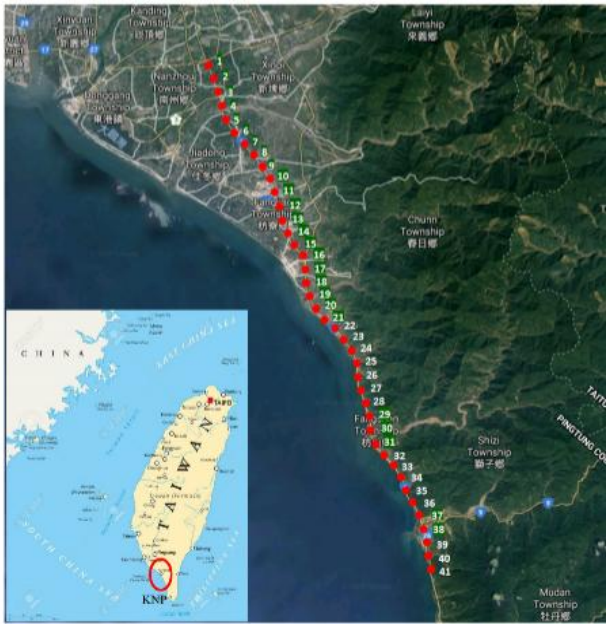

Figure 1 Research road section and onsite survey locations. (Map sources: Google map and town-seek.com)

For the 41-onsite survey locations on the studied road section, several asphalt pavement samples of each location is bring back to laboratory for performing designed tests. The tests include three items; those are (1) asphalt compaction, (2) asphalt content, and (3) asphalt viscosity. For more in detailing descriptions, the compaction of asphalt concrete is the greatest determining factor in dense graded pavement performance. The stiffness, fatigue life, aging, durability, rutting, raveling, and moisture susceptibility, may all be affected by the compaction of asphalt concrete [20]. In this study, the standard test procedure in accordance with CNS 12390 A3288 in is performed [21], to obtain the compaction data for the survey locations. In general, asphalt concrete pavement mixes are typically composed of 5% asphalt cement and 95% aggregates, including stone, sand, and gravel. However, the asphalt content is not a constant value in practical producing processes. As the asphalt content can affect the strength of asphalt concrete, and that may cause pavement damage significantly, so this parameter is tested in this study, according to AASHTO T164 and AASHTO T172. Further, asphalt concrete has a viscoelasticity property, and that is a temperature sensitive material. The viscosity of asphalt mixtures is of particular importance to the forecast of the practical behavior of asphalt concerning the stability in different temperature conditions [22]. Hence, the viscosity of the standard asphalt is measured at 60 ºC based on the descriptions of ASTM Standard D3381-09 and AASHTO M226-80 in this study.

2.2. Pavement Damage Example and Survey Data Pattern

As seen in Figure 2 is examples of asphalt pavement damage, such as sunken, upheave, crack, and pothole, along the road section studied herein. By measuring and calculating onsite pavement damaged-area, in addition to the statistical traffic equivalent as described above, the survey and laboratory test data for the 41 locations is shown in Table 1. As the values of these parameters range quite a large, also as seen in Figure 3, although most data sets exhibit closer to a normal distribution, except the data set of traffic equivalent, those are not all good for analysis from a statistical standpoint. Therefore, it requires a normalization procedure to prevent the effect of extreme values, and for accelerating the convergent speed in neural network calculations [23].

Figure 2 Eamples of asphalt pavement damage along the road section studied herein.

Table -1 Traffic equivalent survey and laboratory test data for the 41 onsite locations

Location	Traffic equivalent	Asphalt compaction (%)	Asphalt content (%)	Asphalt viscosity (×103)	Damaged-area (m2)
1	15174	98.2	4.90	10.8	323
2	15174	99.3	4.60	13.5	156
3	15170	98.5	4.80	9.83	33
4	15179	97.8	4.80	9.83	45
5	15177	98.3	4.80	9.83	27
6	15176	97.5	4.90	8.12	46
7	15178	97.9	5.00	8.12	23
8	15174	98.5	4.80	8.12	64
9	15179	97.3	4.50	25.3	253
10	15180	98.9	4.30	37.5	312
11	15183	97.5	4.60	6.28	41
12	15179	97.6	4.60	5.37	29
13	15185	98.3	4.60	6.33	39

14	15185	96.5	4.90	3.55	29
15	12766	95.8	4.90	3.55	28
16	13018	98.8	5.00	3.52	65
17	10523	96.5	4.90	4.81	96
18	10535	97.7	5.10	4.81	143
19	10533	98.8	5.00	4.81	83
20	10545	98.6	4.90	4.07	57
21	10555	99.5	4.60	4.07	29
22	10600	97.5	4.60	4.07	68
23	10599	96.3	5.00	4.29	29
24	10643	97.8	4.80	4.29	89
25	10750	98.2	5.10	3.7	63
26	11000	96.5	5.10	4.34	44
27	10999	95.3	4.90	4.34	89
28	11051	97.9	5.00	3.9	54
29	11081	98.6	5.00	3.9	78
30	7509	100.5	4.70	23.3	385
31	7519	98.6	5.00	4.42	86
32	7511	99.8	5.00	3.74	31
33	7523	98.9	5.10	4.32	43
34	7529	96.9	5.10	4.32	52
35	7600	97.6	4.70	4.32	57
36	7613	94.5	4.70	33.8	169
37	7595	95.6	4.70	26.5	243
38	7600	97.0	4.70	15.9	47
39	7623	96.8	4.70	16.3	77
40	7600	99.4	4.80	8.6	46
41	7626	98.3	4.90	7.8	25

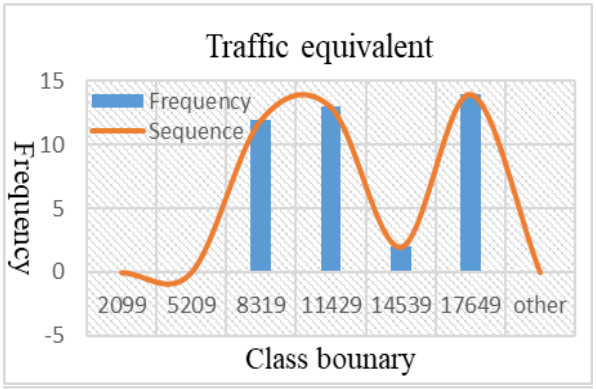

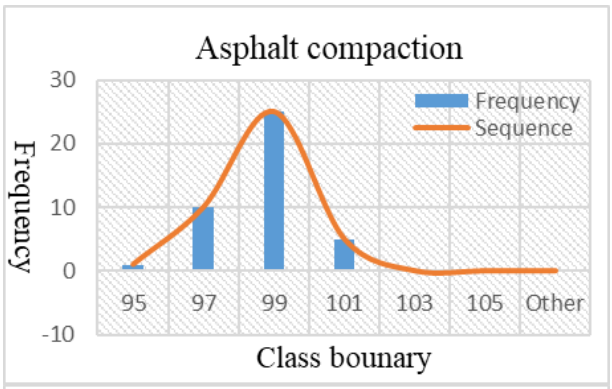

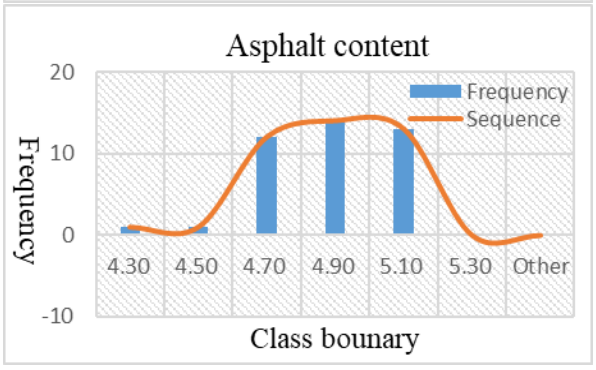

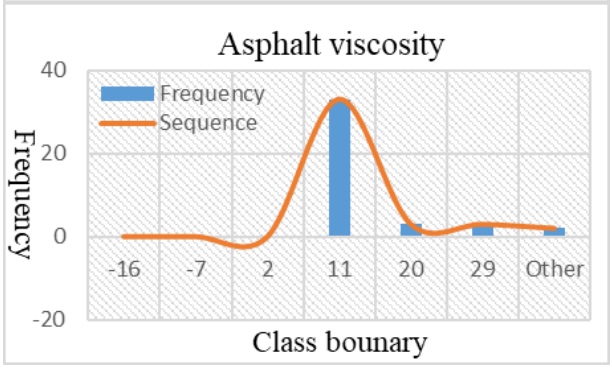

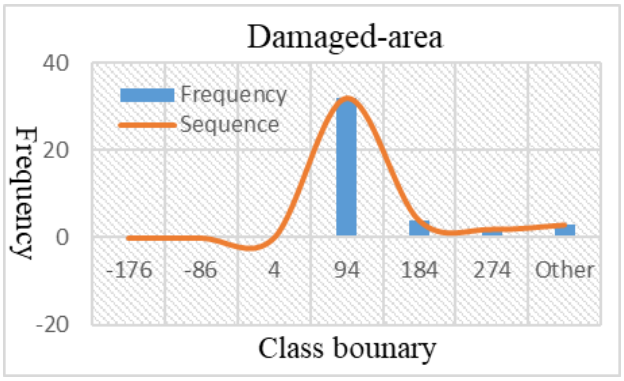

Figure 3 The tendency of normal distribution for the five parameters

In this study, a linear transformation equation is used for all data sets as bellows:

$$t = \frac{(s - s_{min})}{(s_{max} - s_{min})} \tag{1}$$

where t is the value after transformation; s is the value before transformation; smax and smin denote the maximum and the minimum values in the parameter sequence. This formula can guarantee all data have a uniform range between 0 and 1, and that may be good for neural network model development.

III. Neural Network Approach and Evaluation Index

The artificial neural network is one of popular methods used in the field of computational intelligence. There are several types of neural network model [24], but due to the advantages of cost effectiveness and easy to implement in a computer programming, the back-propagation neural network is properly the most common used method in various engineering applications [25-28]. The structure of this supervised learning network model includes an input layer, a hidden layer, and an output layer. The basic equation for this neural network model is:

$$y_j = f(\sum w_{ij} x_i - b_j) \tag{2}$$

where y_j is the output of neuron j; w_{ij} represents the connection weight from neuron i to neuron j; x_i is the input signal generated for neuron i; b_j is the bias term associated with neuron j; and f is the nonlinear transfer function.

This study uses the neural network toolbox of MATLAB to train, verification, and test the data [29]. From documentation in this package, it is known that the back-propagation (BP) neural network is a feedforward network, which updates weight and bias values in general by using Levenberg-Marquardt optimization (trainlm). Alternatively, the process of Bayesian regularization (trainbr), which minimizes a combination of squared errors and weights, and then determines the correct combination to produce a network that generalizes well. Besides, the cascade-forward networks (CN) are similar to feed-forward networks, but include a connection from the input and every previous layer to following layers. Thus, a two-or more layer cascade-network can learn any finite input-output relationship arbitrarily well given enough hidden neurons.

The procedures to perform neural network calculation using MATLAB in the present study may include: (1) Key in “nntool” in data manager to open the main window of neural network toolbox. (2) Import the normalized data sets for input data and target data. (3) Create a new network and select network properties, including network type (BP or CN), training function (trainlm or trainbr), learning function (learngdm), performance function (mse), transfer function (tansig), and set up numbers of layers and neurons. (4) Start to train the data sets with a series of selection of training parameters. (5) Click “performance” to obtain convergent tendency of mean square error, and click “regression” to obtain train, validation, and test results; (6) Back to “nntool” and export the data to save the results.

Different neural network models can generate different learning and estimation results, thus there are three indices including coefficient of determination (R2), coefficient of efficiency (CE), and mean square error (mse), are used to evaluate the performance of neural network calculations. The definitions of these evaluation indices are:

$$R^2 = \left[\sum_{i=1}^{N} (x_i - \bar{x})(y_i - \bar{y}) / \sqrt{\sum_{i=1}^{N} (x_i - \bar{x})^2 \sum_{i=1}^{N} (y_i - \bar{y})^2} \right]^2 \tag{3}$$

$$CE = 1 - \left[\sum_{i=1}^{N} (x_i - y_i)^2 / \sum_{i=1}^{N} (x_i - \bar{x})^2 \right] \tag{4}$$

$$mse = \frac{1}{N}\sum_{i=1}^{N}(x_i - y_i)^2 \tag{5}$$

where x_i is the survey value of number i; y_j is the estimation value of number i; $\overline{x}$ is the averaged value of the total survey data; $\overline{y}$ is the averaged value of the total estimation data; and N is the number of data.

IV. ANALYSIS AND COMPARISON OF COMPUTATIONAL RESULTS

4.1. Neural Network Model

This study uses traffic equivalent (t), asphalt compaction (c), asphalt content (o), and asphalt viscosity (v), as input parameters; meanwhile, uses damaged-area (d) of asphalt pavement as target parameter. To check the sensitivity of each input parameter, there are four types of neural network models, namely Type 1, Type 2, Type 3, and Type 4, as shown in Figure 4, are developed with different combination of these parameters. To determine the number of neurons in the hidden layer, it may use empirical method or try and error method. In this study, the range of neurons is calculate by using the following empirical equation:

$$\frac{(I+O)}{2} \le H_n \le (I+O)\times 2 \tag{6}$$

where I is the number of input parameters; O is the number of output parameter; and Hn is the number of neurons in the hidden layer. For example in this study, in the case of four input parameters (traffic equivalent, asphalt compaction, asphalt viscosity, and asphalt content) and one output parameter (damaged-area), the number of neurons range from three to ten.

4.2. Result Illustration

For the total data sets, the arrangement in the present study are 70%, 15%, and 15% for neural network training, verification, and test, respectively. For Type 1 neural network model, the result of three calculating stages is shown in Table 2. It can be find that the input parameter of asphalt viscosity has the most influence on pavement damaged-area estimation (R2=0.7336), whereas the traffic equivalent (R2=0.2849) and asphalt compaction (R2=0.2844) slight about the same to have the less effect on the estimation. From combinations of two input parameters, as seen in Table 3, the neural network model IovH5Od exhibit to have the highest determination coefficient (R2=0.9049), whereas the neural network model ItoH5Od exhibit to have the least determination coefficient (R2=0.5101). This computational result may imply that the factors of asphalt viscosity and asphalt content are more important in estimating pavement damaged-area.

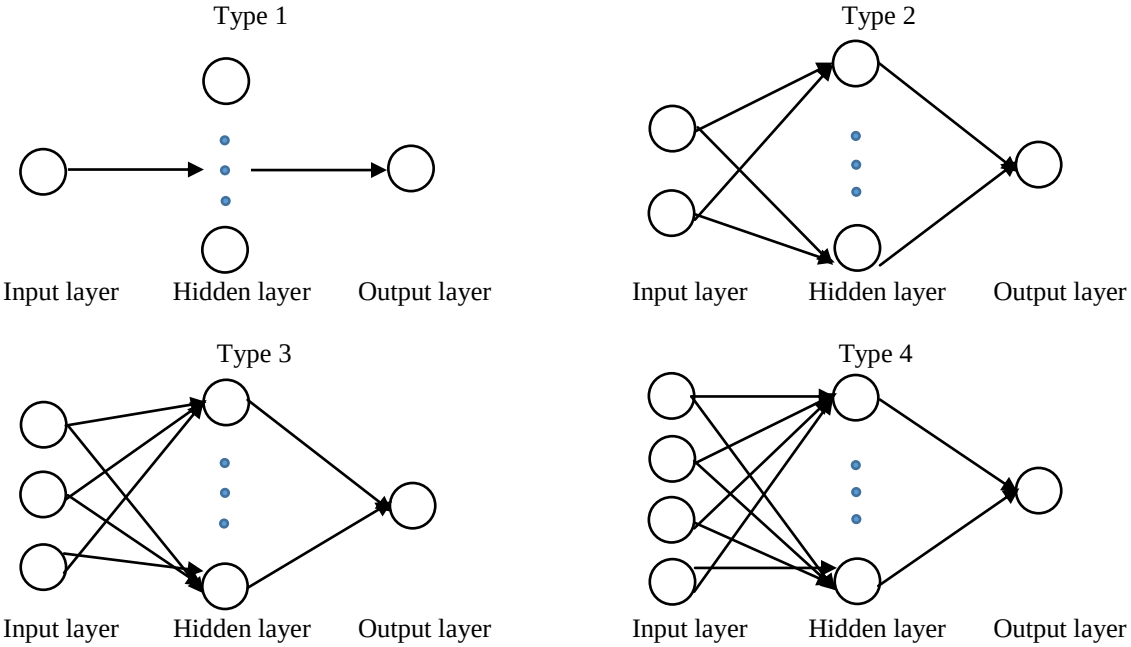

Figure 1 Four different types of neural network model

Table -2 Determination coefficient (R2) of the three calculation stages for Type 1 model

Type 1	Training	Validation	Test	All	Type 1	Training	Validation	Test	All
$I_tH_1O_d$	0.0001	0.0001	0.1852	0.0084	$I_oH_1O_d$	0.1112	0.0031	0.7372	0.2086
$I_tH_2O_d$	0.0022	0.1001	0.4233	0.1726	$I_oH_2O_d$	0.3114	0.0749	0.1529	0.2619
$I_tH_3O_d$	0.3023	0.2172	0.1513	0.2849	$I_oH_3O_d$	0.3037	0.4814	0.7282	0.2006
$I_tH_4O_d$	0.0011	0.3584	0.1867	0.0588	$I_oH_4O_d$	0.5132	0.3496	0.2731	0.3252
$I_cH_1O_d$	0.1780	0.1445	0.1049	0.0147	$I_vH_1O_d$	0.5717	0.8338	0.0692	0.5737
$I_cH_2O_d$	0.4438	0.0854	0.0201	0.2392	$I_vH_2O_d$	0.8397	0.7561	0.4450	0.5643
$I_cH_3O_d$	0.5091	0.0010	0.1499	0.2844	$I_vH_3O_d$	0.5030	0.8353	0.6455	0.5293
$I_cH_4O_d$	0.0030	0.0535	0.0177	0.0185	$I_vH_4O_d$	0.7302	0.7493	0.7256	0.7336

Table -3 Determination coefficient (R2) of the three calculation stages for Type 2 model

Type 2	Training	Validation	Test	All	Type 2	Training	Validation	Test	All
$I_{tc}H_2O_d$	0.1205	0.1524	0.2792	0.0542	$I_{co}H_2O_d$	0.7366	0.0590	0.8759	0.3712
$I_{tc}H_3O_d$	0.1511	0.5851	0.0085	0.1237	$I_{co}H_3O_d$	0.3232	0.2249	0.0952	0.2675
$I_{tc}H_4O_d$	0.4970	0.1913	0.2556	0.3419	$I_{co}H_4O_d$	0.6489	0.6010	0.2803	0.4733
$I_{tc}H_5O_d$	0.1813	0.1330	0.2005	0.1505	$I_{co}H_5O_d$	0.6608	0.6747	0.9584	0.6458
$I_{tc}H_6O_d$	0.9551	0.8123	0.2969	0.5603	$I_{co}H_6O_d$	0.5180	0.8903	0.8455	0.5774
$I_{to}H_2O_d$	0.1282	0.2757	0.0227	0.1235	$I_{cv}H_2O_d$	0.6533	0.8903	0.0003	0.6644
$I_{to}H_3O_d$	0.4975	0.0344	0.0232	0.3568	$I_{cv}H_3O_d$	0.7097	0.4558	0.7946	0.6129
$I_{to}H_4O_d$	0.2589	0.8285	0.3283	0.3818	$I_{cv}H_4O_d$	0.3588	0.8362	0.9222	0.6994
$I_{to}H_5O_d$	0.5932	0.5154	0.5239	0.5101	$I_{cv}H_5O_d$	0.5330	0.9188	0.7022	0.5436
$I_{to}H_6O_d$	0.6201	0.2660	0.2524	0.4523	$I_{cv}H_6O_d$	0.5727	0.9991	0.2400	0.5795
$I_{tv}H_2O_d$	0.3034	0.2318	0.8688	0.4355	$I_{ov}H_2O_d$	0.7785	0.0581	0.5485	0.7347
$I_{tv}H_3O_d$	0.8881	0.8688	0.7943	0.8313	$I_{ov}H_3O_d$	0.5863	0.4638	0.0986	0.5679
$I_{tv}H_4O_d$	0.8135	0.6344	0.8806	0.6583	$I_{ov}H_4O_d$	0.5014	0.7960	0.7070	0.5646
$I_{tv}H_5O_d$	0.3746	0.7590	0.3219	0.3456	$I_{ov}H_5O_d$	0.9302	0.9094	0.9787	0.9049
$I_{tv}H_6O_d$	0.9536	0.9073	0.2414	0.7521	$I_{ov}H_6O_d$	0.7839	0.5398	0.8736	0.6625

The above results show that the factor of asphalt viscosity has a more influence than that of asphalt content on estimating pavement damaged-area. The other two factors may also affect the calculation, although these factors are not that much of influence, they are unneglectable. To improve the model performance, the result for three combinations of the four input parameters is displayed in Table 4. The neural network model ItovH4Od has the best performance with a determination coefficient of R2=0.9437. Thus, the parameter of traffic equivalent is the third important factor to affect the model performance. At last, for the all four input parameters, the calculating result is exhibited in Table 5. The neural network model ItcovH6Od, with a determination coefficient of R2=0.9669, performs better than that of the other models, including all of previous models. The performance and convergent tendency of each calculation stage for this preferred model is shown in Figure 5 and Figure 6, respectively. These results present a very high correlation coefficient and small mean square error between survey data and estimation result. Therefore, it may conclude that all the four input parameters do have an influence on pavement damaged-area estimation, but the importance in descending order are asphalt viscosity, asphalt content, traffic equivalent, and asphalt compaction. This information may be useful for related government agency to consider road maintenances.

Table -4 Determination coefficient (R2) of the three calculation stages for Type 3 model

Type 3	Training	Validation	Test	All	Type 3	Training	Validation	Test	All
$I_{tco}H_2O_d$	0.3248	0.0496	0.1706	0.2367	$I_{tov}H_2O_d$	0.7677	0.8407	0.8347	0.7428
$I_{tco}H_3O_d$	0.5115	0.0955	0.2916	0.3623	$I_{tov}H_3O_d$	0.8383	0.9804	0.9676	0.8647
$I_{tco}H_4O_d$	0.7477	0.9296	0.6478	0.7108	$I_{tov}H_4O_d$	0.9106	0.9964	0.9577	0.9437
$I_{tco}H_5O_d$	0.9702	0.8134	0.9019	0.9310	$I_{tov}H_5O_d$	0.9583	0.9575	0.5366	0.9239
$I_{tco}H_6O_d$	0.7843	0.4877	0.3041	0.4547	$I_{tov}H_6O_d$	0.8048	0.9732	0.9654	0.9021
$I_{tco}H_7O_d$	0.6794	0.9782	0.4951	0.6658	$I_{tov}H_7O_d$	0.9390	0.9271	0.8904	0.9315
$I_{tco}H_8O_d$	0.9913	0.9715	0.5063	0.7736	$I_{tov}H_8O_d$	0.6336	0.9164	0.4064	0.6823
$I_{cov}H_2O_d$	0.9057	0.7471	0.9970	0.8639	$I_{tcv}H_2O_d$	0.6224	0.7625	0.6566	0.6564

$I_{cov}H_3O_d$	0.8772	0.9532	0.9257	0.8989	$I_{tcv}H_3O_d$	0.6092	0.4590	0.0422	0.5559
$I_{cov}H_4O_d$	0.9048	0.8196	0.8902	0.8683	$I_{tcv}H_4O_d$	0.3999	0.8062	0.9239	0.5517
$I_{cov}H_5O_d$	0.9066	0.9649	0.3919	0.8732	$I_{tcv}H_5O_d$	0.8306	0.9397	0.9313	0.8367
$I_{cov}H_6O_d$	0.8460	0.3168	0.8973	0.7878	$I_{tcv}H_6O_d$	0.5579	0.9688	0.4281	0.5795
$I_{cov}H_7O_d$	0.7875	0.5019	0.6710	0.6349	$I_{tcv}H_7O_d$	0.4422	0.3544	0.1192	0.4039
$I_{cov}H_8O_d$	0.9407	0.8981	0.2999	0.6686	$I_{tcv}H_8O_d$	0.9484	0.9700	0.1671	0.9047

Table -5 Determination coefficient (R2) of the three calculation stages for Type 4 model

Type 4	Training	Validation	Test	All	Type 4	Training	Validation	Test	All
$I_{tcov}H_3O_d$	0.9703	0.9003	0.1365	0.9386	$I_{tcov}H_7O_d$	0.7109	0.9756	0.8703	0.8827
$I_{tcov}H_4O_d$	0.8610	0.9738	0.5501	0.8568	$I_{tcov}H_8O_d$	0.8988	0.9226	0.7872	0.8447
$I_{tcov}H_5O_d$	0.9568	0.9993	0.7370	0.9599	$I_{tcov}H_9O_d$	0.7523	0.8183	0.5817	0.7646
$I_{tcov}H_6O_d$	0.9622	0.9985	0.9968	0.9669	$I_{tcov}H_{10}O_d$	0.6575	0.9850	0.9831	0.7343

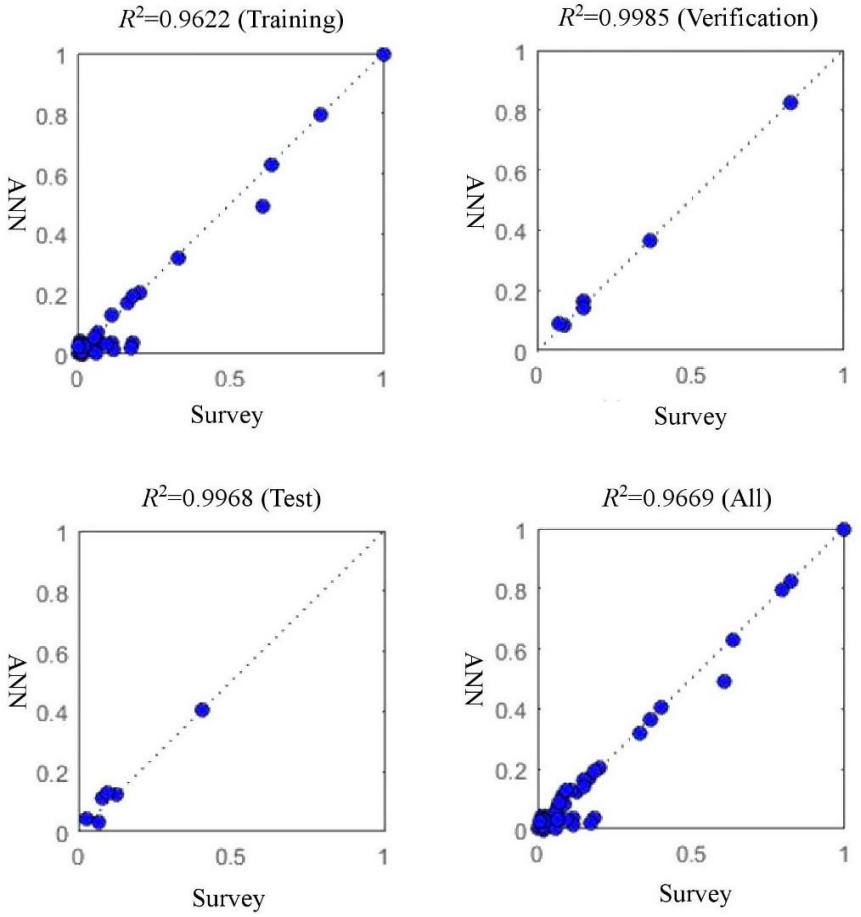

Figure 5. Correlation between survey data and neural network estimation

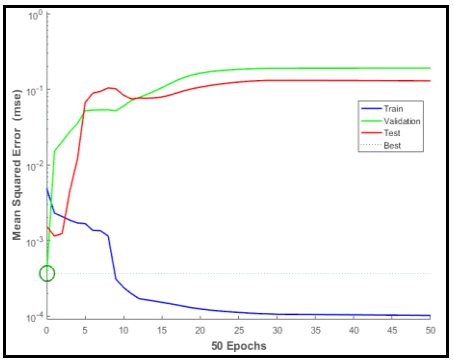

Figure 6. Convergent tendency of each neural network calculation stage

For checking to see if there is any other way to improve the performance of the best model discussed above, in the following, the cascade-forward networks and the process of Bayesian regularization, are introduced and compared to enhance further the model development. After a series of training, verification, and test neural network models with different neurons in the hidden layer, the performance of a relatively better model for each network with training function is presented in Table 6. It can be found that the model ItcovH6Od has the highest determination coefficient for all the data set. Also, because the nonlinearity of linking those parameters with different dimensions, the efficiency coefficient is adequately to use in here and present in the table. Again, the model ItcovH6Od has the highest efficiency coefficient (CE=0.9450), which is closer to 1.0. That is, this neural network model has a good quality and acceptable reliability, the weight and bias term is shown in Table 7, and that may be applicable to other road sections of interest.

Table - 6 Comparison of different neural network models with different training functions

BP/trainlm	R2 (Training)	R2 (Validation)	R2 (Test)	R2 (All)	CE (All)
$I_{tcov}H_6O_d$	0.9622	0.9985	0.9968	0.9669	0.9450
BP/trainbr					
$I_{tcov}H_6O_d$	0.6720	0.7766	0.9507	0.7111	0.8068
CN/trainlm					
$I_{tcov}H_7O_d$	0.8926	0.9530	0.7965	0.9262	0.7132
CN/trainbr					
$I_{tcov}H_4O_d$	0.5392	0.9406	0.9290	0.6634	0.6323

Table - 7 The weight and bias term of the developed neural network model ItcovH6Od

w{1,1}	1	2	3	4	b{1}	w{2,1}	b{2}
1	1.17680	-2.64300	0.14600	-2.27780	-3.44450	-0.34131	-0.38050
2	0.39677	-1.69940	1.58350	-2.16110	-0.69928	-0.07524	-
3	1.65210	1.27690	0.93241	-0.66182	-0.50985	0.14639	-
4	-0.33759	0.97338	-1.39680	2.02750	-0.38846	0.78060	-
5	-0.82773	0.92119	-0.69229	0.81262	-2.37850	0.26741	-
6	-2.30770	-1.68610	1.23660	0.88727	-2.41400	-0.20453	-

V.CONCLUSION

With increasing of asphalt road construction as well as increasing of traffic volume in Taiwan highway system, the road surface damage often occurs. Based on the onsite survey and laboratory test result, this study taken four parameters including statistical traffic equivalent, asphalt compaction, asphalt content, and asphalt viscosity in the input layer, and varied different number of neurons in the hidden layer, to develop a neural network model for estimating pavement damaged-area in the output layer.

In accordance with the evaluation indices, such as determination coefficient, mean square error, and efficiency coefficient, the comparison results from a series of model development, showed that the model ItcovH6Od of using back-propagation network with Levenberg-Marquardt optimization have the best performance. Although the present study used only 41 available data sets to develop the model, it believed to satisfy a minimum sense of 30 data sets from a statistical point of view. Therefore, the developed neural network model should have a sufficient reliability, and the proposed method could be applicable in other road sections of interest.

For future study, the using of more data sets, as well as consider other factors such as temperature, rain accumulation, and road pavement thickness in the training process of neural network model, might be performed to increase its reliability and applicability. Nevertheless, this study provided a new way and acceptable result to predict asphalt pavement damage-area, and that might be useful for road maintenance and traffic safety management in the field of highway engineering.

Acknowledgements: The authors would like to thank Mr. Sianbin Pan, who works at the Third Maintenance Office, Directorate General of Highways in Taiwan, to provide onsite traffic survey and asphalt laboratory test data.

VI. REFERENCES

[1] Y.Y. Chien, "Burning billions of roads, road blood drop state compensation record," http://www.yuyen.tw/2011/12/blog-post_05.html, 2011.
[2] F.L. Roberts, P.S. Kandhal, E.R. Brown, D.Y. Lee, T.W. Kennedy, "Hot mix asphalt materials, mixture design, and construction," NAPA Education Foundation, Lanham, Maryland, USA, 1996.
[3] K.Y. Lin, "Effect of different additives on the characteristics of asphalt mastics," Ph.D. Dissertation, National Cheng Kung University, Tainan, Taiwan, 2006.
[4] J.S. Chen, C.H. Wang, "Development of asphalt concrete oil content specification limits allowance by statistical method," Taiwan Highway Engineering, Vol.36, No.10, pp. 2-23, 2010.
[5] J.S. Chen, W.T. Liu, M.C. Liao, C.H. Wang, Y.C. Tsai, H.C. Lin, "Analysis of causing pavement pothole and maintenance method recommendation," Taiwan Highway Engineering, Vol.37, No.10, pp. 2-47, 2011.
[6] H. Zakeri, F.M. Nejad, A. Fahimifar, "A quadcopter unmanned aerial vehicle based on a systematic mage processing approach toward an automated asphalt pavement inspection," Automation in Construction, Vol. 72, pp. 21-23, 2016.
[7] A.Tedeschi, F. Benedetto, "A real-time automatic pavement crack and pothole recognition system for mobile android-based devices," Advanced Engineering Informatics, Vol. 32, pp. 11-25, 2017.
[8] T.H. Bullock, M.V.L. Bennett, D. Johnston, R. Josephson, E. Marder, R.D. Fields, "The neuron doctrine," Science, Vol. 310, pp. 791-793, 2005.
[9] B. Doll, H. Ozer, J. Rivera-Perez, I.I. Al-Qadi, J. Lambros, "Damage zone development in heterogeneous asphalt concrete," Engineering Fracture Mechanics, Vol. 182, pp. 356-371, 2017.
[10] A. Sha, S. Tu, "Cracks characteristics and damage mechanism of asphalt pavement with semi-rigid base," The 7th RILEM International Conference on Cracking in Pavements, pp. 985-995, 2012.
[11] M.I. Hossain, R.A. Tarefder, "Determining damage effects on asphalt concrete composites," International Journal of Civil and Structural Engineering, Vol. 3, No 4, pp. 692-703, 2013.
[12] Onifade, B. Birgisson, "Damage and fracture characterization of asphalt concrete mixtures using the equivalent micro-crack stress approach," Construction and Building Materials, Vol. 148, pp. 521-530, 2017.
[13] L. Sun, G. Wang, H. Zhang, L. Liu, "Initiation and propagation of top-down cracking in asphalt pavement," Applied Sciences, doi:10.3390/app8050774, pp. 1-14, 2018.
[14] H. Sharma, A.K. Swamy, "Development of probabilistic fatigue curve for asphalt concrete based on viscoelastic continuum damage mechanics," International Journal of Pavement Research and Technology, Vol. 9, No. 4, pp. 270-279, 2016.
[15] H. Faisal, R. Tarefder, M. Weldegiorgis, "Nanoindentation characterization of moisture damage in different phases of asphalt concrete," Advances in Civil Engineering Materials, Vol. 4, No. 1, pp. 31-46, 2015.
[16] Z. Tong, J. Gao, Z. Han, Z. Wang, "Recognition of asphalt pavement crack length using deep convolutional neural networks," Journal of Road Materials and Pavement Design, Vol. 19, No. 6, pp. 1334-1349, 2016.
[17] Y.X. Huang, F., Shao, Y.W. Liu, "Damage condition assessment of expressway asphalt pavement based on RBF neural network," Advanced Materials Research, Vol. 446-449, pp. 2548-2553, 2012.
[18] P. Ghasemi, M. Aslani, D.K. Rollins, R.C., Williams, V.R. Schaefer, "Modeling rutting susceptibility of asphalt pavement using principal component pseudo inputs in regression and neural networks," International Journal of Pavement Research and Technology, https://doi.org/10.1016/j.ijprt.2018.01.003, pp. 1-12, 2018.
[19] Directorate General of Highways, "Statistical tables of highway traffic volume investigations," Ministry of Transportation and Communications, Taiwan, https://www.thb.gov.tw/sites/ch/modules/download/download_list?node=bcc520be3e03-4e28-b4cb7e338ed6d9b d&c =83baff80-2d7f-4a66-9285-d989f48effb4, 2016.
[20] C.S. Hughes, "National cooperative highway research program synthesis of highway practice 152: compaction of asphalt pavement," Transportation Research Board, National Research Council, Washington, D.C., USA, 1989.
[21] Public Construction Commission,"Asphalt concrete pavement," Construction Outline Code of Public Constructio, Chap. 02742, pp. 02742-10, 2014.
[22] Schellenberg, H.J. Eulitz, K. Paschke, "Determination of the viscosity of bitumen or mortar measured by the tensile retardation test (ReVis)," The 6th Eurasphalt & Eurobitume Congress, Prague, Czech Republic, http://dx.doi.org/10.14311/EE.2016.164, pp. 1-9, 2016.
[23] MATLAB, " Technical forum," Matlab Electric Journal, Vol. 5, pp. 6-33, 2011.
[24] Y.C. Yeh, "Neural network model - application and practice," Rulin Book Company, Taiwan, 1993.
[25] A. Heidari, M. Hashempour, D. Tavakoli, "Using of backpropagation neural network in estimating of compressive strength of waste concrete," Soft Computing in Civil Engineering, Vol. 1, No. 1, pp. 54-64, 2017.
[26] Faghri, J. Hua, "Evaluation of artificial neural network applications in transportation engineering," Transportation Research Board, National Research Council, Washington D.C., Record 1358, pp. 71-80, 1992.
[27] Mahmoudi, M.A. Arjomand, M. Rezaei, M.H. Mohammadi, "Predicting the earthquake magnitude using the multilayer perceptron neural network with two hidden layers," Civil Engineering Journal, Vol. 2, No. 1, pp. 1-12, 2016.
[28] D. Park, L.R. Rilett, "Forecasting freeway link travel times with a multilayer feedforward neural network," Computer-Aided Civil and Infrastructure Engineering, Vol. 14, No. 5, pp. 357-367, 1999.
[29] MATLAB, "Documentation support," The MathWorks, Inc., USA, https://www.mathworks.com/help/nnet/, 2018.